Experimental Neurology 338 (2021) 113607

Contents lists available at ScienceDirect

Experimental Neurology

journal homepage: www.elsevier.com/locate/yexnr

Research paper

Protection against oxaliplatin-induced mechanical and thermal hypersensitivity in *Sarm1*$^{-/-}$ mice

Stacey Anne Gould [a,b], Matthew White [b,c], Anna L. Wilbrey [d], Erzsébet Pór [e], Michael Philip Coleman [a,b], Robert Adalbert [a,b,e,*]

[a] John van Geest Centre for Brain Repair, University of Cambridge, Cambridge, UK
[b] The Babraham Institute, Cambridge, UK
[c] Department of Basic and Clinical Neuroscience, The Maurice Wohl Clinical Neuroscience Institute, Institute of Psychiatry, Psychology and Neuroscience (IoPPN), King's College London, London SE5 9RT, UK
[d] Wellcome Sanger Institute, Wellcome Genome Campus, Hinxton, Cambridge CB10 1SA, UK
[e] Department of Anatomy, Histology and Embryology, Faculty of Medicine, University of Szeged, Szeged H-6724, Hungary

ARTICLE INFO

Keywords:
Oxaliplatin
WLD^S
SARM1
Mechanical hypersensitivity
Cold hypersensitivity
Neuropathic pain
Axon degeneration

ABSTRACT

Chemotherapy-induced peripheral neuropathy (CIPN) is a common dose-limiting side effect of cancer treatment, often associated with degeneration of sensory axons or their terminal regions. Presence of the slow Wallerian degeneration protein (WLD^S), or genetic deletion of sterile alpha and TIR motif containing protein 1 (SARM1), which strongly protect axons from degeneration after injury or axonal transport block, alleviate pain in several CIPN models. However, oxaliplatin can cause an acute pain response, suggesting a different mechanism of pain generation. Here, we tested whether the presence of WLD^S or absence of SARM1 protects against acute oxaliplatin-induced pain in mice after a single oxaliplatin injection. In BL/6 and *Wld*^{S} mice, oxaliplatin induced significant mechanical and cold hypersensitivities which were absent in *Sarm1*$^{-/-}$ mice. Despite the presence of hypersensitivity there was no significant loss of intraepidermal nerve fibers (IENFs) in the footpads of any mice after oxaliplatin treatment, suggesting that early stages of pain hypersensitivity could be independent of axon degeneration. To identify other changes that could underlie the pain response, RNA sequencing was carried out in DRGs from treated and control mice of each genotype. *Sarm1*$^{-/-}$ mice had fewer gene expression changes than either BL/6 or *Wld*^{S} mice. This is consistent with the pain measurements in demonstrating that *Sarm1*$^{-/-}$ DRGs remain relatively unchanged after oxaliplatin treatment, unlike those in BL/6 and *Wld*^{S} mice. Changes in levels of four transcripts – *Alas2, Hba-a1, Hba-a2,* and *Tfrc* – correlated with oxaliplatin-induced pain, or absence thereof, across the three genotypes. Our findings suggest that targeting SARM1 could be a viable therapeutic approach to prevent oxaliplatin-induced acute neuropathic pain.

1. Introduction

Ongoing pain caused by chemotherapy-induced peripheral neuropathy (CIPN) worsens quality of life of in patients undergoing chemotherapy (Farquhar-smith, 2016). This makes CIPN a common dose-limiting side effect of diverse chemotherapeutic agents. Oxaliplatin, used against most solid cancers, causes a distal dose-dependent symmetrical 'glove and stocking' type painful sensory neuropathy, comprising numbness, tingling and burning sensations (Chiorazzi et al., 2015; Kanat et al., 2017). Acute, transient neuropathies manifest in 90% of patients within 24–48 h of oxaliplatin infusion (Cersosimo, 2005; Starobova and Vetter, 2017) with symptoms exacerbated by exposure to cool temperatures (Argyriou et al., 2013).

Studies in patients and animal models implicate axonal degeneration as a common process in CIPN pathology (Fukuda et al., 2017), where chemotherapeutic drugs directly or indirectly trigger a "dying back" axon degeneration that progresses in a distal-to-proximal manner. This type of programmed axon death also occurs after acute injury (Waller,

Abbreviations: Alas2, aminolevulinic acid synthase 2 erythroid; Hba-a1, haemoglobin alpha adult chain 1; Hba-a2, haemoglobin alpha adult chain 2; Hbb, haemoglobin beta; Tfrc, transferrin receptor; CCCP, carbonyl cyanide *m*-chlorophenyl hydrazine; OIPN, oxaliplatin-induced peripheral neuropathy; TRPM2, transient receptor potential melastatin 2; ADPR, ADP-ribose; cADPR, cyclic ADP-ribose; NMNAT2, nicotinamide mononucleotide adenylyltransferase 2..

* Corresponding author at: Department of Anatomy, Histology and Embryology, Faculty of Medicine, University of Szeged, Szeged H-6724, Hungary.
E-mail address: adalbert.janos.robert@med.u-szeged.hu (R. Adalbert).

https://doi.org/10.1016/j.expneurol.2021.113607
Received 14 October 2020; Received in revised form 7 January 2021; Accepted 9 January 2021
Available online 15 January 2021

1850) and in many disease models (Coleman and Hoke, 2020; Conforti et al., 2014), including pain. *Wld*^{S} mice, which possess a spontaneous mutation that slows programmed axon death (Adalbert et al., 2005; Buckmaster et al., 1995; Mack et al., 2001), exhibit weaker thermal hyperalgesia and decreased mechanical allodynia after painful chronic constriction injury compared to wild-type injured mice (Myers et al., 1996; Ramer and Bisby, 1997; Ramer and Bisby, 1997; Sommer and Schafers, 1998). Furthermore, WLD^S-expressing axons are protected against vincristine-induced degeneration *in vitro* (Wang et al., 2001) and paclitaxel-induced neuropathy *in vivo* (Wang et al., 2002), suggesting that peripheral nerves may undergo programmed axon death in the presence of some chemotherapeutic agents. Likewise, removal of pro-degenerative protein sterile alpha and TIR motif containing 1 (SARM1) has a similar robust protective efficacy as WLD^S after injury (Osterloh et al., 2012) and in models of CIPN induced by vincristine, paclitaxel, and bortezomib (Geisler et al., 2019a; Geisler et al., 2016; Turkiew et al., 2017).

Proposed mechanisms for chemotherapy-induced axon degeneration by different chemotherapeutics include; altered axon transport and axon degeneration by vincristine and paclitaxel (Boyette-Davis et al., 2013; LaPointe et al., 2013; Siau et al., 2006), altered mitochondrial function and Ca^{2+} homeostasis (Fukuda et al., 2017), and bortezomib-induced transcriptional changes leading to SARM1 activation (Geisler et al., 2019b) in addition to its microtubule-targeting properties (Pero et al., 2019). The mechanism of oxaliplatin-induced pain is unclear. Whilst OIPN could be due to axon degeneration, symptoms in patients receiving oxaliplatin tend to subside between treatment cycles (Extra et al., 1998) and can completely resolve after cessation of treatment (Kanat et al., 2017) suggesting involvement of non-degenerative pain-inducing mechanisms.

After rapid non-enzymatic conversion of oxaliplatin to oxalate and a platinum-containing derivative (Starobova and Vetter, 2017), the oxalate moiety induces cold-hypersensitivity, whereas the platinum-containing derivative induces mechanical allodynia in rats (Sakurai et al., 2009). Platinum compounds accumulate in dorsal root ganglia (DRGs), where they form DNA adducts (Faivre et al., 2003). Therefore, damage to nuclear or mitochondrial DNA in DRGs or other cells, or other (unknown) actions of platinum-based compounds could underlie the acute pain response.

Here we investigated whether the presence of WLD^S or absence of SARM1 protects against acute oxaliplatin-induced pain in mice. Cold and mechanical sensitivity, as well as assessing intraepidermal nerve fiber (IENF) density as a readout of distal axon degeneration were employed, and transcriptional changes were observed *via* RNA Sequencing. We demonstrate that acute oxaliplatin-treatment induced significant mechanical and cold hypersensitivity in wild-type mice. This was attenuated in *Sarm1*$^{-/-}$ mice but not in *Wld*^{S} mice. Hypersensitivities were not associated with detectable loss of IENFs in footpads of any genotype after oxaliplatin treatment which suggests that the early stages of pain hypersensitivity may be independent of axon degeneration. However, we noted transcriptional changes that correlate with induction of pain phenotypes.

2. Material and methods

2.1. Animals

All animal work was undertaken at the Babraham Institute in accordance with the Animals (Scientific Procedures) Act 1986 under project licence number 70/7620. Wild-type C57BL/6Babr (BL/6), *Wld*^{S} and *Sarm1*$^{-/-}$ male mice (both on a C57BL/Babr background) aged 12–16 weeks were used for the study. Mice were housed under controlled conditions (12 h light-dark cycle) in individually ventilated cages (IVCs) in a pathogen-free environment with standard rodent chow and water available *ad libitum* (except when behavioural assessments were being made). Most mice were group housed (2–3 mice per cage), though very occasionally a mouse was housed individually.

2.2. Oxaliplatin administration

We assessed behaviour and intraepidermal nerve fiber (IENF) density after administration of a single intraperitoneal (i.p.) 6 mg/kg oxaliplatin injection as previously described (Descoeur et al., 2011; Young et al., 2014), outlined in Supplementary Fig. 1. Oxaliplatin (Sigma-Aldrich) was dissolved in 0.9% sodium chloride (AppliChem).

2.3. Behavioural tests

Mechanical allodynia was assessed using a dynamic plantar aesthesiometer and thermal allodynia using a dynamic cold plate. For the plantar aesthesiometer test, mice were placed into individual sections of a plastic box with a wire mesh floor and left to habituate for 30–60 min. Then, a dynamic plantar aesthesiometer (Ugo Basile) was used to apply pressure up to a maximum of 5 g at a rate of 0.5 g/s to the plantar region of the right hind paw. If the mouse did not withdraw its paw after 30 s, the experiment was stopped manually and the probe retracted. This was repeated five times with at least 10 min between each measurement. The average of the five values for each mouse was taken forward for analysis. This was repeated 48 h after oxaliplatin administration. For the cold plate test, an individual mouse was placed onto a dynamic hot/cold plate (Ugo Basile) at 18 °C. The plate was cooled at a rate of 0.3 °C/min to 2 °C and the number of jumps (defined as both rear paws off the plate simultaneously) was recorded and grouped into 2 °C bins (Young et al., 2014). The baseline measurement is the number of jumps prior to oxaliplatin injection. This process was repeated 4 days after mice received the injection to obtain the post-oxaliplatin measurements, based on a previous study which noted that cold sensitivity peaked 4 days after oxaliplatin administration (Young et al., 2014). We refer to this as allodynia (rather than hyperalgesia) since in our mice, no increase in jumping behaviour was observed at lower temperatures before oxaliplatin administration, suggesting these temperatures are not painful in naïve mice. Cold plate data is presented as the area under the curve alongside individual time courses.

2.4. Sample sizes and exclusions

In all behavioural studies, group sizes were 12 mice. Control vehicle-treated groups were also included. No wild-type or *Sarm1*$^{-/-}$ mice were excluded from any of the studies. One *Wld*^{S} mouse was excluded from the study as it performed abnormally in the cold plate test at baseline compared to the other mice. The mouse was excluded from all successive assessments (including other behavioural tests and histological assessment of intraepidermal nerve fiber density).

2.5. Epidermal nerve fiber analysis

Evaluation of intraepidermal innervation (IENF) was performed using immunohistochemical staining for PGP 9.5, a pan-axonal marker, as described previously (Melli et al., 2006). Briefly, 4 days post-injection, 2 mm punch biopsies were taken from the medial footpads of the right hind limb and fixed in PLP fixative. After cryosectioning, the slides were stained with anti-PGP 9.5 antibody (Sigma-Aldrich AB5925). IENFs were counted in 4–6 sections for each mouse and averaged. The data were presented as the mean number of fibers per linear millimetre of epidermis.

2.6. RNA Sequencing

2.6.1. Animals

Mice of three experimental genotypes (C57BL/6Babr, *Wld*^{s} and *Sarm1*$^{-/-}$ −; $n = 8$ animals per genotype) were processed for transcriptomic studies. Two-month-old mice were administered either a

single intraperitoneal injection of 6 mg/kg oxaliplatin or saline ($n = 4$ mice per treatment).

2.6.2. RNA isolation

Dorsal root ganglia (L3-L5) were sub dissected in RNase-free conditions (RNaseZap, Sigma Aldrich) from freshly culled mice and flash frozen until further use. For RNA extraction, tissue was thawed directly in TRIsure reagent (Bioline) and RNA isolated following manufacturer's instructions. RNA was purified (RNeasy kit, Qiagen) with on-column DNase treatment and analysed on an Agilent 2100 Bioanalyzer.

2.6.3. RNA-seq library preparation

Only RNA samples with RIN > 8 were used for sequencing. Libraries were prepared using the TruSeq (unstranded) mRNA kit (Illumina) following the manufacturer's low sample protocol. Following library amplification and bead purification, the final fragment size was analysed, and libraries quantified using the Universal KAPA Library Quantification kit (Kapa Biosystems) and a Bio-Rad C100 thermal cycler. An equal amount of cDNA was used to pool up to four samples, which were sequenced in one lane. Sequencing was carried out to a depth of 20 million 25-bp single-end reads per library.

2.6.4. Bioinformatics pipeline and statistics

FastQ files were trimmed with Trim Galore v0.4.3 using default settings then aligned against the mouse GRCm38 genome assembly with hisat2 v2.0.5 using options –no-mixed and –no-discordant. Mapped positions with MAPQ values of < 20 were discarded.

Gene expression was quantified using the RNA-Seq quantification

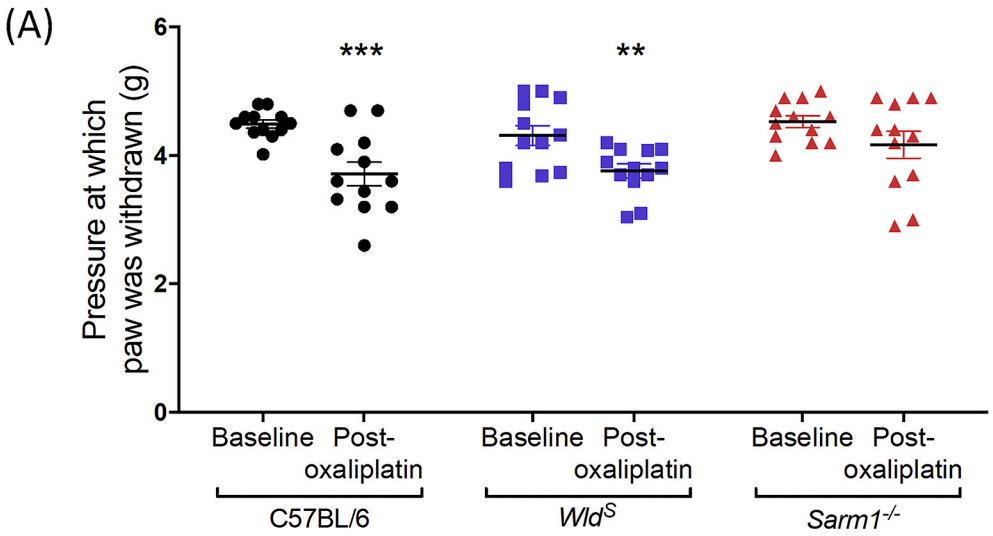

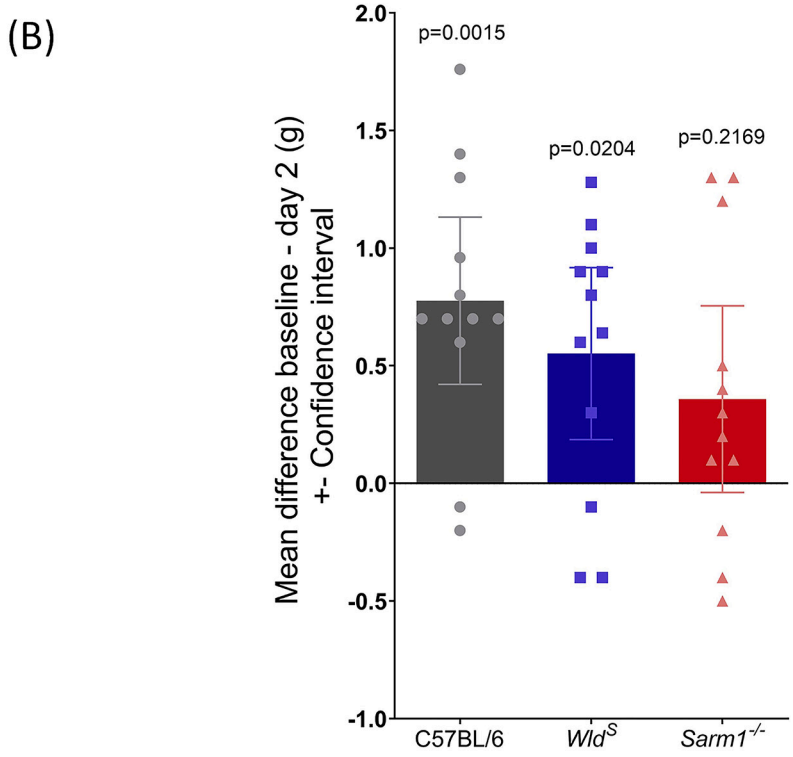

Fig. 1. Tactile sensitivity observed in BL/6, *Wld*^{S}and *Sarm1*$^{-/-}$mice between baseline and 2 days after oxaliplatin administration. (A) Both BL/6 and *Wld*^{S}, but not *Sarm1*$^{-/-}$ mice exhibit increased mechanical hypersensitivity when pressure was applied to the paw using the plantar aesthesiometer. Statistically significant difference between groups is indicated (***$p < 0.001$; **$p < 0.01$, two-way ANOVA followed by Sidak's post-hoc pairwise comparison). (B) Mean difference in mechanical hypersensitivity between baseline and 2 days post-oxaliplatin treatment for the three genotypes. *P* values are shown on the graph, with statistically significant difference for BL/6 and *Wld*^{S} (paired *t*-tests followed by Bonferroni correction for multiple comparisons). Data are presented as mean ± s.e.m. $n = 12$ per group.

pipeline in SeqMonk v1.37.0 in unstranded library mode using gene models from Ensembl v67. For count based statistics, raw read counts over exons in each gene were used. For visualization and other statistics, log2 RPM (reads per million reads of library) expression values were used.

Differentially expressed genes were selected using pairwise comparisons with DESeq2 with a cut-off of $P < 0.05$ following multiple testing correction. A secondary intensity filter akin to a dynamic fold-change filter was applied to DESeq2 hits. DESeq2 comparisons were between saline and oxaliplatin treated mice of each experimental genotype.

2.7. Statistical analysis

Microsoft Excel was used to store raw data and calculate mean values. Statistical analysis and graphical visualisations were made using GraphPad Prism 6 (USA). For cold plate analysis, a Mann Whitney test followed by Bonferroni analysis was performed on area under the curve (AUC) data. For the plantar aesthesiometer, two-way ANOVA followed by Sidak's multiple comparison test was used (for Fig. 1.A) in order to identify and quantify differences between genotypes and/or treatment overall. For Fig. 1.B, mean difference in mechanical hypersensitivity was analysed using paired *t*-tests followed by Bonferroni correction for

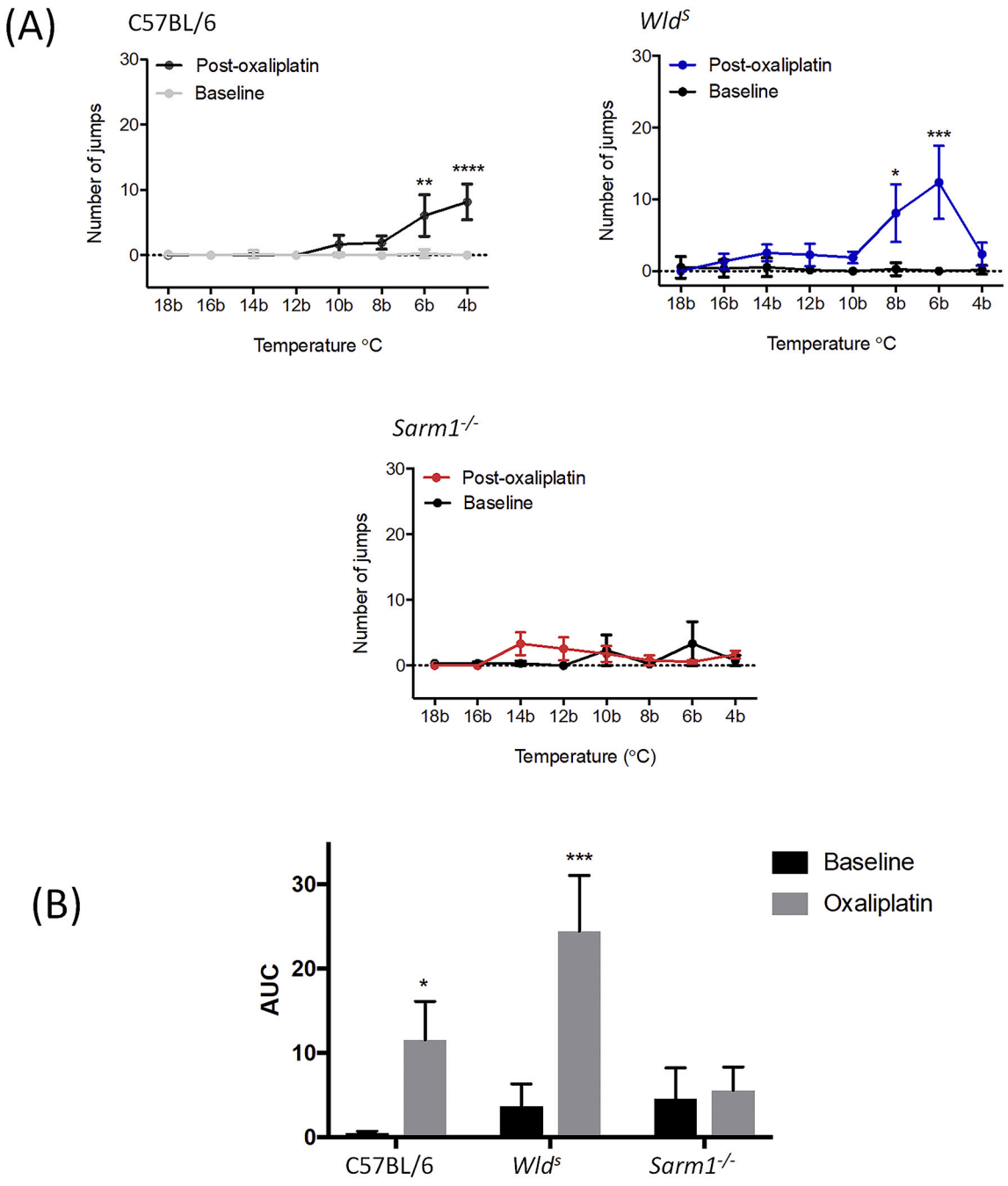

Fig. 2. Oxaliplatin-induced cold hypersensitivity is prevented by removal of SARM1, but not the presence of WLD^S. (A) Number of jumps made by BL/6, *Wld*^{S} and *Sarm1*$^{-/-}$ mice in response to a cold ramp (cooling from 18 °C to 2 °C) before (baseline) and 4 days after a single dose of oxaliplatin. (B) BL/6 and *Wld*^{S} mice exhibit a significant increase in the number of jumps after oxaliplatin treatment while there is no change in *Sarm1*$^{-/-}$ mice. Statistically significant difference between groups is indicated (*$p < 0.05$ and *** $p < 0.001$, AUC-area under the curve showing difference in the total number of jumps in response to declining temperature ramp from 18 °C to 2 °C). Data are presented as mean ± s.e.m. n = 12 per group.

multiple comparisons. For assessment of intraepidermal nerve fiber density, two-way ANOVA followed by Sidak's multiple comparison test was used.

3. Results

The present study has assessed thermal and mechanical allodynia (tested on different days to minimise interference between testing sessions; Supplementary Fig. 1) and intraepidermal nerve fiber (IENF) density after a single administration of oxaliplatin *in vivo*. Changes to RNA expression were also assessed after oxaliplatin administration.

3.1. Sarm1 deletion blocks the development of mechanical hypersensitivity following acute oxaliplatin treatment

In order to assess whether absence of SARM1 or presence of WLD^S protects against mechanical allodynia, following acute oxaliplatin treatment, we injected all three mouse genotypes with a single dose of oxaliplatin (6 mg/kg). Forty-eight hours after oxaliplatin administration, wild-type and *Wld*^{S} mice displayed increased sensitivity to pressure; they withdrew their paws at a significantly lower pressure than they did at baseline assessment (Fig. 1.A, B). Remarkably, the *Sarm1*$^{-/-}$ mice displayed no significant difference in sensitivity to pressure as their threshold for removing their paws was the same as baseline (Fig. 1.A, B). None of the three genotypes tested differed significantly in the pressure they withdrew their paws at baseline assessment (Fig. 1.A).

3.2. Sarm1 deletion prevents the development of cold hypersensitivity following acute oxaliplatin treatment

At baseline, there was no difference in cold-induced jumping behaviour of wild-type, *Wld*^{S} or *Sarm1*$^{-/-}$ mice at any of the temperatures measured. However, 4 days after a single 6 mg/kg injection of oxaliplatin, wild-type mice showed significantly increased jumping compared to baseline measures (Fig. 2.A, B). Similarly, *Wld*^{S} mice exhibited significantly increased jumping behaviour after oxaliplatin treatment compared to baseline and this increase was greater than that seen in the wild-type mice (Fig. 2.A, B). Interestingly, the jumping behaviour of *Sarm1*$^{-/-}$ did not change from baseline after oxaliplatin treatment (Fig. 2.A, B).

3.3. Acute oxaliplatin treatment does not induce intraepidermal nerve fiber (IENF) loss

There was no difference in IENF density between the three genotypes treated with saline (Fig. 3). No change in IENF density was detected for any genotypes post-oxaliplatin treatment. Although we cannot exclude highly localised effects outside the regions studied, this suggests that general axon degeneration does not underpin the pain phenotype after acute oxaliplatin administration.

3.4. RNA expression changes after acute oxaliplatin administration

To explore the mechanistic link between acute oxaliplatin treatment and differences in behaviour we collected RNA from dorsal root ganglia (DRGs) of mice treated with either saline or oxaliplatin (4 days after treatment). Mice used for the RNA sequencing study exhibited similar levels of mechanical allodynia as those used in the behavioural and histological studies (Supplementary Fig. 2). DRGs were chosen for RNA Sequencing as they have previously been implicated in the pathophysiology of the oxaliplatin pain mechanism. We hypothesised that acute oxaliplatin treatment would induce changes in DRG gene expression that are either a consequence of pathological events or could even be part of the pathogenic mechanism in both mechanical and cold hypersensitivity observed in these animals. Transcriptomic differences between C57BL/6, *Wld*^{S} and *Sarm1*$^{-/-}$ mice in response to oxaliplatin treatment could

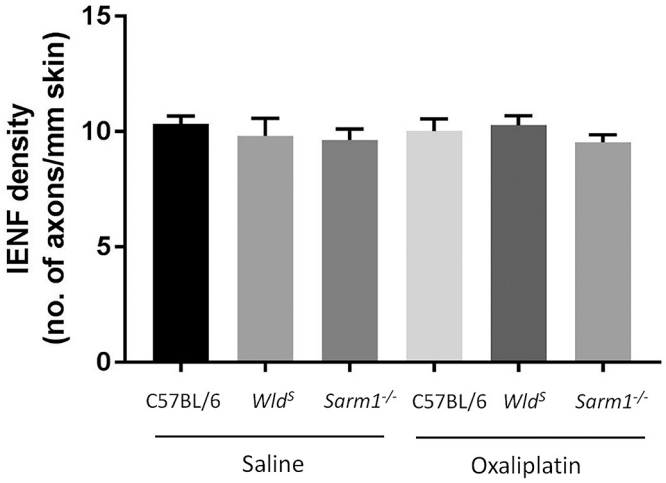

Fig. 3. A single dose of oxaliplatin (6 mg/kg) does not induce degeneration of intraepidermal nerve fibers (IENF) 4 days after treatment. IENF density of BL/6, *Wld*^{S} and *Sarm1*$^{-/-}$ mice after acute oxaliplatin administration remains unchanged when mice are treated with saline (vehicle injections) or oxaliplatin.

underlie the differences seen in pain response and the resistance of *Sarm1*$^{-/-}$ mice to cold and mechanical hypersensitivity.

Following acute oxaliplatin treatment we observed 46 differentially expressed genes in wild-type mice relative to saline treatment (Fig. 4.A). This included 26 upregulated and 20 downregulated genes. The number of differentially expressed genes in *Wld*^{S} mice in response to oxaliplatin treatment was lower with a total of 4 upregulated and 9 downregulated genes (Fig. 4.A). Consistent with the absence of significant behavioural changes, only three differentially expressed genes were noted in *Sarm1*$^{-/-}$ mice following treatment with oxaliplatin (Fig. 4.A) and these genes were not shared with either C57BL/6 or *Wld*^{S} mice (Fig. 4.B). This lack of transcriptomic perturbation in *Sarm1*$^{-/-}$ mice is in keeping with their resistance to oxaliplatin-induced mechanical and cold hypersensitivity. Decreased expression of four transcripts correlated with oxaliplatin-induced pain across the three genotypes: *Alas2, Hba-a1, Hba-a2,* and *Tfrc*. (Fig. 4.C).

4. Discussion

Here, using a previously described protocol (Young et al., 2014), we report that acute oxaliplatin administration induces mechanical and cold hypersensitivities in wild-type (BL/6) and *Wld*^{S} mice. This reflects acute peripheral neuropathies comprising cold-induced paraesthesia, dysaesthesia and pain that appear abruptly after administration in the clinic (Cersosimo, 2005). We associate acute oxaliplatin-induced pain with a plethora of transcriptional changes without loss of intraepidermal nerve fibers (IENFs) in BL/6 and *Wld*^{S} mice. Genetic deletion of *Sarm1* prevents development of these acute painful neuropathies and transcriptional changes are largely absent in DRGs from *Sarm1*$^{-/-}$-oxaliplatin-treated mice. The lack of detectable IENF loss in any genotype, and the absence of protection against pain in *Wld*^{S} mice suggest a mechanism of pain generation independent from programmed axon death. In support of this, no known genes involved in programmed neurone or axon death were identified through our RNA sequencing. The common transcriptional changes occurring in mice that developed pain were downregulation of four iron metabolism and haem synthesis genes: *Alas2*, *Hba-a1*, *Hba-a2*, and *Tfrc*. A full list of gene expression changes observed in each genotype can be viewed in Supplementary Table 1.

While *Alas2*, *Hba-a1*, *Hba-a2*, and *Tfrc* have known functions in erythrocytes, the absence of altered erythroid-specific gene expression, *GATA binding protein 1* (*Gata1*) and *erythroid-associated factor* (*Eraf*), or endothelial specific genes, CD34 and Vascular Endothelial Growth

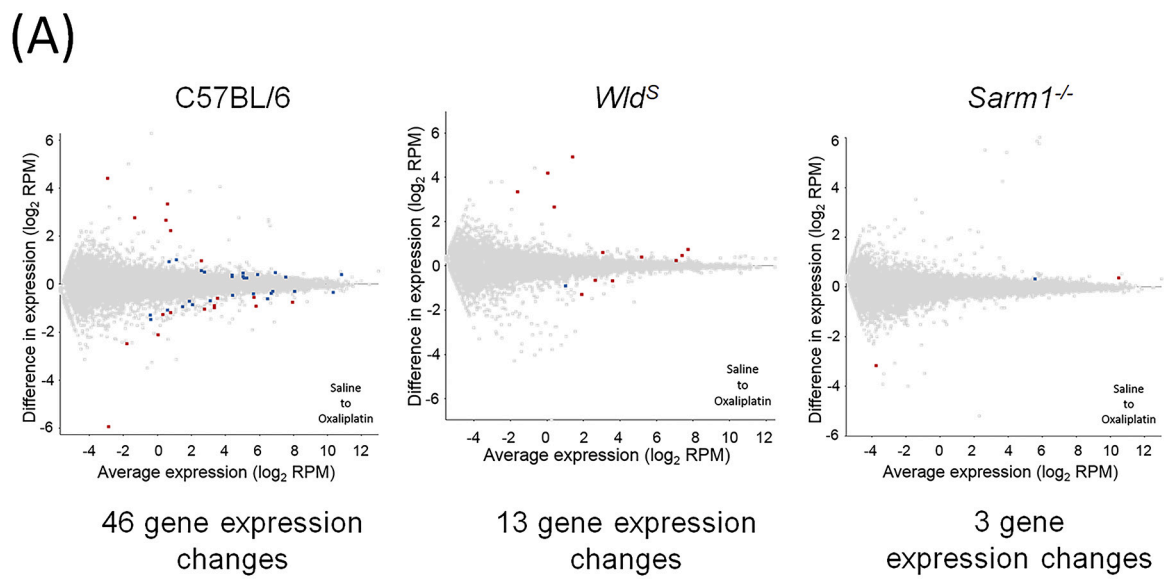

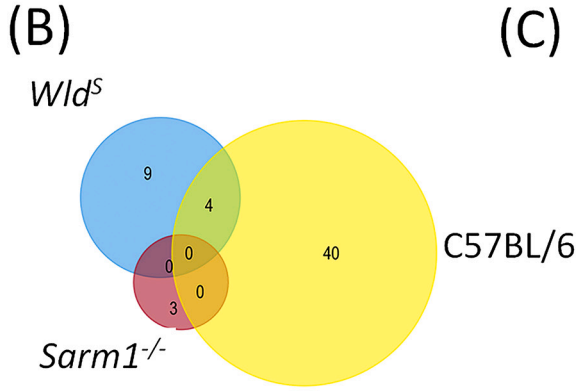

(C)

Feature	Description	Fold Change C57B/6 Saline vs oxaliplatin	Fold Change Wld^S Saline vs oxaliplatin
Alas2	aminolevulinic acid synthase 2, erythroid	6.8	10.1
Hba-a1	hemoglobin alpha, adult chain 1	10.2	18.4
Hba-a2	hemoglobin alpha, adult chain 2	4.7	6.3
Tfrc	transferrin receptor	1.4	1.2

Fig. 4. RNA Sequencing identified common genes downregulated in BL/6 and *Wld*^{S}mice that were not differentially expressed in *Sarm1*$^{-/-}$mice. (A) M (log ratio)–A (mean average) plots of significantly differentially expressed genes (DEGs) in DRGs of BL/6, *Wld*^{S} and *Sarm1*$^{-/-}$ mice after treatment with oxaliplatin (RPM, reads per million reads of input). Comparison: DESeq2 (differential gene expression analysis based on negative binomial distribution) saline *vs.* oxaliplatin treatment ($n = 4$ mice per treatment per genotype). Blue dots indicate significant changes (DESeq2) and red dots indicate significant changes that are also intensity hits. (B) Venn diagram highlighting overlapping DEGs between BL/6, *Wld*^{S} and *Sarm1*$^{-/-}$ mice after treatment with oxaliplatin. (C) Common DEGs in BL/6, and *Wld*^{S} mice following oxaliplatin treatment are highlighted. All differentially expressed genes are listed in Supplementary Table 1.

Factor Receptor 2 (KDR), indicate that differential gene expression was not due to contamination by erythrocytes (Richter et al., 2009; Vanni et al., 2018). Interestingly, literature describes roles of ALAS2 and haemoglobin in central and peripheral neurones, including DRGs (Biagioli et al., 2009; Haraguchi et al., 2011; Richter et al., 2009; Stephens et al., 2019; Walser et al., 2017). Genetic mutations in *Alas2*, haemoglobin, and *Tfrc* genes have been observed in patients with painful or neurodegenerative conditions (Bishop et al., 2013; Kallianpur et al., 2014; Vanni et al., 2018): Haemoglobin in human brain (Biagioli et al., 2009; Richter et al., 2009) is differentially expressed in frontal cortex of humans with prion-related neurodegenerative diseases (Vanni et al., 2018). Mouse models of depression and chronic stress exhibit increased expression of *Alas2* (Stankiewicz et al., 2015; Stankiewicz et al., 2014; Yamamoto et al., 2015). Animal models of pain show that chemotherapeutic paclitaxel causes downregulation of *Hba* and *Hbb* in rat DRGs (Nishida et al., 2008), and there is an association between chronic constriction injury-induced neuropathic pain with downregulation of *Alas2*, *Hba-a1*, and *Hba-a2* (amongst other genes) in DRGs of female mice (Stephens et al., 2019). This evidence along with changes we noted in our acute OIPN model supports a role of *Alas2*, *Hba-a1*, and *Hba-a2* downregulation in painful neuropathies. However, whether these are causal or reflect other pathogenic events is a crucial question for future studies to address.

Oxaliplatin accumulates in rat DRG mitochondria (Nishida et al., 2018) causing downregulation of mitochondrial electron transport chain proteins and increased reactive oxygen species (ROS) which is associated with oxaliplatin-induced mechanical allodynia (Cheng et al., 2019). Since *Alas2*, *Hba-a1*, and *Hba-a2* are important for mitochondrial function, their downregulation could indicate mitochondrial stress. Indeed, mitochondrial toxin rotenone causes transcriptional downregulation of neuronal haemoglobin genes *Hba-a2* and *Hbb* in rats (Richter et al., 2009). Removal of SARM1 protects against axon degeneration triggered by mitochondrial toxins rotenone and CCCP (Loreto et al., 2020; Summers et al., 2014) and sub-degenerative concentrations of CCCP induce SARM1 activation without causing degeneration (Sasaki et al., 2020). Taken together, we speculate that removal of SARM1 could protect against oxaliplatin-induced mitochondrial dysfunction associated with SARM1 activation in a context that leads to pain in the absence of axon degeneration.

Oxaliplatin forms protein adducts with many proteins (Graham et al.,

2000; Pendyala and Creaven, 1993) and oxaliplatin-haemoglobin adducts have been shown to affect cytoplasmic pH and sensitise TRP channels in DRGs (Peng et al., 2005; Potenzieri et al., 2020). Activation of TRP channels is associated with pain (Jang et al., 2018), including oxaliplatin-induced mechanical allodynia (Sakurai et al., 2009), and mice lacking TRPM2 exhibit decreased mechanical allodynia after paclitaxel (So et al., 2015). SARM1 products ADPR and cADPR (Essuman et al., 2017; Horsefield et al., 2019) can activate the TRPM2 channel (Yu et al., 2019). Therefore, another speculative pathway through which SARM1 may act in pre-degeneration pain pathophysiology could be TRP channel activation or sensitisation *via* SARM1 products.

Finally, SARM1 is also reported as a positive regulator of cytokine and chemokine production in the innate immune system (Hou et al., 2013; Szretter et al., 2009; Wang et al., 2018). Acute oxaliplatin treatment increases C—C chemokine ligand 2 (CCL2) in small rat DRGs whereas its receptor (CCR2) is increased in medium and large DRGs, associated with mechanical hypersensitivity (Illias et al., 2018). However, a recent study questions the extent to which SARM1 is truly involved in mediating cytokine responses (Uccellini et al., 2020) and no altered chemokine RNA transcripts were associated with acute oxaliplatin administration in the present study. However, the heterogeneity of our DRG population could confound our ability to detect altered transcription that may occur in specific DRG sub-types, of which there are 11 possessing distinct mRNA profiles (Li et al., 2016; Usoskin et al., 2015).

5. Conclusions

The present study contributes data towards an emerging role of *Alas2*, *Hba-a1*, and *Hba-a2* gene downregulation in pain pathophysiology and a role of SARM1 in acute chemotherapy-induced peripheral neuropathy. This work raises several interesting questions which future studies should address, including: Do these gene expression changes drive pain pathophysiology or are they a consequence of mitochondrial dysfunction or other pathological changes? What role does SARM1 activation have in the absence of programmed axon death? Are other axonal proteins such as tubulin or pro-survival protein NMNAT2 modified in the presence of oxaliplatin and do they play a causative role in CIPN?

Supplementary data to this article can be found online at https://doi.org/10.1016/j.expneurol.2021.113607.

Funding

This work was supported by the United Kingdom Medical Research Council project grant (MR/L003813/1); Biotechnology and Biological Sciences Research Council Institute Strategic Programme Grant; and the John and Lucille van Geest Foundation.

Declaration of Competing Interest

None.

Acknowledgements

We would like to thank Anne Segonds-Pichon for assistance with statistical analysis, Simon Andrews for assistance with analysis of RNA-seq data and the Babraham Institute Experimental Unit staff for technical assistance.

References

Adalbert, R., Gillingwater, T.H., Haley, J.E., Bridge, K., Beirowski, B., Berek, L., Wagner, D., Grumme, D., Thomson, D., Celik, A., Addicks, K., Ribchester, R.R., Coleman, M.P., 2005. A rat model of slow Wallerian degeneration (WldS) with improved preservation of neuromuscular synapses. Eur. J. Neurosci. 21, 271–277.

Argyriou, A.A., Cavaletti, G., Antonacopoulou, A., Genazzani, A.A., Briani, C., Bruna, J., Terrazzino, S., Velasco, R., Alberti, P., Campagnolo, M., Lonardi, S., Cortinovis, D., Cazzaniga, M., Santos, C., Psaromyalou, A., Angelopoulou, A., Kalofonos, H.P., 2013. Voltage-gated sodium channel polymorphisms play a pivotal role in the development of oxaliplatin-induced peripheral neurotoxicity: results from a prospective multicenter study. Cancer 119, 3570–3577.

Biagioli, M., Pinto, M., Cesselli, D., Zaninello, M., Lazarevic, D., Roncaglia, P., Simone, R., Vlachouli, C., Plessy, C., Bertin, N., Beltrami, A., Kobayashi, K., Gallo, V., Santoro, C., Ferrer, I., Rivella, S., Beltrami, C.A., Carninci, P., Raviola, E., Gustincich, S., 2009. Unexpected expression of alpha- and beta-globin in mesencephalic dopaminergic neurons and glial cells. Proc. Natl. Acad. Sci. U. S. A. 106, 15454–15459.

Bishop, D.F., Tchaikovskii, V., Nazarenko, I., Desnick, R.J., 2013. Molecular expression and characterization of erythroid-specific 5-aminolevulinate synthase gain-of-function mutations causing X-linked protoporphyria. Mol. Med. 19, 18–25.

Boyette-Davis, J.A., Cata, J.P., Driver, L.C., Novy, D.M., Bruel, B.M., Mooring, D.L., Wendelschafer-Crabb, G., Kennedy, W.R., Dougherty, P.M., 2013. Persistent chemoneuropathy in patients receiving the plant alkaloids paclitaxel and vincristine. Cancer Chemother. Pharmacol. 71, 619–626.

Buckmaster, E.A., Perry, V.H., Brown, M.C., 1995. The rate of Wallerian degeneration in cultured neurons from wild type and C57BL/WldS mice depends on time in culture and may be extended in the presence of elevated K+ levels. Eur. J. Neurosci. 7, 1596–1602.

Cersosimo, R.J., 2005. Oxaliplatin-associated neuropathy: a review. Ann. Pharmacother. 39, 128–135.

Cheng, W., Xiang, W., Wang, S., Xu, K., 2019. Tanshinone IIA ameliorates oxaliplatin-induced neurotoxicity via mitochondrial protection and autophagy promotion. Am. J. Transl. Res. 3140–3149.

Chiorazzi, A., Semperboni, S., Marmiroli, P., 2015. Current view in platinum drug mechanisms of peripheral neurotoxicity. Toxics 3, 304–321.

Coleman, M.P., Hoke, A., 2020. Programmed axon degeneration: from mouse to mechanism to medicine. Nat. Rev. Neurosci. 21, 183–196.

Conforti, L., Gilley, J., Coleman, M.P., 2014. Wallerian degeneration: an emerging axon death pathway linking injury and disease. Nat. Rev. Neurosci. 15, 394–409.

Descoeur, J., Pereira, V., Pizzoccaro, A., Francois, A., Ling, B., Maffre, V., Couette, B., Busserolles, J., Courteix, C., Noel, J., Lazdunski, M., Eschalier, A., Authier, N., Bourinet, E., 2011. Oxaliplatin-induced cold hypersensitivity is due to remodelling of ion channel expression in nociceptors. EMBO Mol. Med. 3, 266–278.

Essuman, K., Summers, D.W., Sasaki, Y., Mao, X., DiAntonio, A., Milbrandt, J., 2017. The SARM1 toll/Interleukin-1 receptor domain possesses intrinsic NAD(+) cleavage activity that promotes pathological axonal degeneration. Neuron 93 (1334–1343), e1335.

Extra, J.M., Marty, M., Brienza, S., Misset, J.L., 1998. Pharmacokinetics and safety profile of oxaliplatin. Semin. Oncol. 25, 13–22.

Faivre, S., Chan, D., Salinas, R., Woynarowska, B., Woynarowski, J.M., 2003. DNA strand breaks and apoptosis induced by oxaliplatin in cancer cells. Biochem. Pharmacol. 66, 225–237.

Farquhar-smith, P., 2016. Persistent Pain in Cancer Survivors: Pathogenesis and Treatment Options.

Fukuda, Y., Li, Y., Segal, R.A., 2017. A mechanistic understanding of axon degeneration in chemotherapy-induced peripheral neuropathy. Front. Neurosci. 11, 481.

Geisler, S., Doan, R.A., Strickland, A., Huang, X., Milbrandt, J., DiAntonio, A., 2016. Prevention of vincristine-induced peripheral neuropathy by genetic deletion of SARM1 in mice. Brain 139, 3092–3108.

Geisler, S., Doan, R.A., Cheng, G.C., Cetinkaya-Fisgin, A., Huang, S.X., Hoke, A., Milbrandt, J., DiAntonio, A., 2019a. Vincristine and bortezomib use distinct upstream mechanisms to activate a common SARM1-dependent axon degeneration program. JCI Insight. 4.

Geisler, S., Huang, S.X., Strickland, A., Doan, R.A., Summers, D.W., Mao, X., Park, J., DiAntonio, A., Milbrandt, J., 2019b. Gene therapy targeting SARM1 blocks pathological axon degeneration in mice. J. Exp. Med. 216, 294–303.

Graham, M.A., Lockwood, G.F., Greenslade, D., Brienza, S., Bayssas, M., Gamelin, E., 2000. Clinical pharmacokinetics of oxaliplatin: a critical review. Clin. Cancer Res. 6, 1205–1218.

Haraguchi, T., Yanaka, N., Eguchi, Y., Kudo, T., Hirata, A., Kato, N., 2011. Fish oil feeding up-regulates the expression of 5-aminolevulinate synthase 2 mRNA in rat brain. Biosci. Biotechnol. Biochem. 75, 1383–1385.

Horsefield, S., Burdett, H., Zhang, X., Manik, M.K., Shi, Y., Chen, J., Qi, T., Gilley, J., Lai, J.S., Rank, M.X., Casey, L.W., Gu, W., Ericsson, D.J., Foley, G., Hughes, R.O., Bosanac, T., von Itzstein, M., Rathjen, J.P., Nanson, J.D., Boden, M., Dry, I.B., Williams, S.J., Staskawicz, B.J., Coleman, M.P., Ve, T., Dodds, P.N., Kobe, B., 2019. NAD(+) cleavage activity by animal and plant TIR domains in cell death pathways. Science 365, 793–799.

Hou, Y.J., Banerjee, R., Thomas, B., Nathan, C., Garcia-Sastre, A., Ding, A., Uccellini, M. B., 2013. SARM is required for neuronal injury and cytokine production in response to central nervous system viral infection. J. Immunol. 191, 875–883.

Illias, A.M., Gist, A.C., Zhang, H., Kosturakis, A.K., Dougherty, P.M., 2018. Chemokine CCL2 and its receptor CCR2 in the dorsal root ganglion contribute to oxaliplatin-induced mechanical hypersensitivity. Pain 159, 1308–1316.

Jang, Y., Cho, P.S., Yang, Y.D., Hwang, S.W., 2018. Nociceptive roles of TRPM2 Ion Channel in pathologic pain. Mol. Neurobiol. 55, 6589–6600.

Kallianpur, A.R., Jia, P., Ellis, R.J., Zhao, Z., Bloss, C., Wen, W., Marra, C.M., Hulgan, T., Simpson, D.M., Morgello, S., McArthur, J.C., Clifford, D.B., Collier, A.C., Gelman, B. B., McCutchan, J.A., Franklin, D., Samuels, D.C., Rosario, D., Holzinger, E., Murdock, D.G., Letendre, S., Grant, I., Group, C.S, 2014. Genetic variation in iron

metabolism is associated with neuropathic pain and pain severity in HIV-infected patients on antiretroviral therapy. PLoS One 9, e103123.
Kanat, O., Ertas, H., Caner, B., 2017. Platinum-induced neurotoxicity: a review of possible mechanisms. World J. Clin. Oncol. 8, 329–335.
LaPointe, N.E., Morfini, G., Brady, S.T., Feinstein, S.C., Wilson, L., Jordan, M.A., 2013. Effects of eribulin, vincristine, paclitaxel and ixabepilone on fast axonal transport and kinesin-1 driven microtubule gliding: implications for chemotherapy-induced peripheral neuropathy. Neurotoxicology 37, 231–239.
Li, C.L., Li, K.C., Wu, D., Chen, Y., Luo, H., Zhao, J.R., Wang, S.S., Sun, M.M., Lu, Y.J., Zhong, Y.Q., Hu, X.Y., Hou, R., Zhou, B.B., Bao, L., Xiao, H.S., Zhang, X., 2016. Somatosensory neuron types identified by high-coverage single-cell RNA-sequencing and functional heterogeneity. Cell Res. 26, 83–102.
Loreto, A., Hill, C.S., Hewitt, V.L., Orsomando, G., Angeletti, C., Gilley, J., Lucci, C., Sanchez-Martinez, A., Whitworth, A.J., Conforti, L., Dajas-Bailador, F., Coleman, M. P., 2020. Mitochondrial impairment activates the Wallerian pathway through depletion of NMNAT2 leading to SARM1-dependent axon degeneration. Neurobiol. Dis. 134, 104678.
Mack, T.G., Reiner, M., Beirowski, B., Mi, W., Emanuelli, M., Wagner, D., Thomson, D., Gillingwater, T., Court, F., Conforti, L., Fernando, F.S., Tarlton, A., Andressen, C., Addicks, K., Magni, G., Ribchester, R.R., Perry, V.H., Coleman, M.P., 2001. Wallerian degeneration of injured axons and synapses is delayed by a Ube4b/Nmnat chimeric gene. Nat. Neurosci. 4, 1199–1206.
Melli, G., Jack, C., Lambrinos, G.L., Ringkamp, M., Hoke, A., 2006. Erythropoietin protects sensory axons against paclitaxel-induced distal degeneration. Neurobiol. Dis. 24, 525–530.
Myers, R.R., Heckman, H.M., Rodriguez, M., 1996. Reduced hyperalgesia in nerve-injured WLD mice: relationship to nerve fiber phagocytosis, axonal degeneration, and regeneration in normal mice. Exp. Neurol. 141, 94–101.
Nishida, K., Kuchiiwa, S., Oiso, S., Futagawa, T., Masuda, S., Takeda, Y., Yamada, K., 2008. Up-regulation of matrix metalloproteinase-3 in the dorsal root ganglion of rats with paclitaxel-induced neuropathy. Cancer Sci. 99, 1618–1625.
Nishida, K., Takeuchi, K., Hosoda, A., Sugano, S., Morisaki, E., Ohishi, A., Nagasawa, K., 2018. Ergothioneine ameliorates oxaliplatin-induced peripheral neuropathy in rats. Life Sci. 207, 516–524.
Osterloh, J.M., Yang, J., Rooney, T.M., Fox, A.N., Adalbert, R., Powell, E.H., Sheehan, A. E., Avery, M.A., Hackett, R., Logan, M.A., MacDonald, J.M., Ziegenfuss, J.S., Milde, S., Hou, Y.J., Nathan, C., Ding, A., Brown Jr., R.H., Conforti, L., Coleman, M., Tessier-Lavigne, M., Zuchner, S., Freeman, M.R., 2012. dSarm/Sarm1 is required for activation of an injury-induced axon death pathway. Science 337, 481–484.
Pendyala, L., Creaven, P.J., 1993. In vitro cytotoxicity, protein binding, red blood cell partitioning, and biotransformation of oxaliplatin. Cancer Res. 53, 5970–5976.
Peng, J., Mandal, R., Sawyer, M., Li, X.F., 2005. Characterization of intact hemoglobin and oxaliplatin interaction by nanoelectrospray ionization tandem mass spectrometry. Clin. Chem. 51, 2274–2281.
Pero, M.E., Meregalli, C., Qu, X., Kumar, A., Shorey, M., Rolls, M., Tanji, K., Brannagan, T.H., Alberti, P., Fumagalli, G., Monza, L., Cavaletti, G., Bartolini, F., 2019. Pathogenic role of Delta 2 tubulin in Bortezomib induced peripheral neuropathy. bioRxiv 721852.
Potenzieri, A., Riva, B., Rigolio, R., Chiorazzi, A., Pozzi, E., Ballarini, E., Cavaletti, G., Genazzani, A.A., 2020. Oxaliplatin-induced neuropathy occurs through impairment of haemoglobin proton buffering and is reversed by carbonic anhydrase inhibitors. Pain 161, 405–415.
Ramer, M.S., Bisby, M.A., 1997. Rapid sprouting of sympathetic axons in dorsal root ganglia of rats with a chronic constriction injury. PAIN 70, 237–244.
Richter, F., Meurers, B.H., Zhu, C., Medvedeva, V.P., Chesselet, M.F., 2009. Neurons express hemoglobin alpha- and beta-chains in rat and human brains. J. Comp. Neurol. 515, 538–547.
Sakurai, M., Egashira, N., Kawashiri, T., Yano, T., Ikesue, H., Oishi, R., 2009. Oxaliplatin-induced neuropathy in the rat: involvement of oxalate in cold hyperalgesia but not mechanical allodynia. Pain 147, 165–174.
Sasaki, Y., Engber, T.M., Hughes, R.O., Figley, M.D., Wu, T., Bosanac, T., Devraj, R., Milbrandt, J., Krauss, R., DiAntonio, A., 2020. cADPR is a gene dosage-sensitive biomarker of SARM1 activity in healthy, compromised, and degenerating axons. Exp. Neurol. 329, 113252.
Siau, C., Xiao, W., Bennett, G.J., 2006. Paclitaxel- and vincristine-evoked painful peripheral neuropathies: loss of epidermal innervation and activation of Langerhans cells. Exp. Neurol. 201, 507–514.
So, K., Haraguchi, K., Asakura, K., Isami, K., Sakimoto, S., Shirakawa, H., Mori, Y., Nakagawa, T., Kaneko, S., 2015. Involvement of TRPM2 in a wide range of inflammatory and neuropathic pain mouse models. J. Pharmacol. Sci. 127, 237–243.
Sommer, C., Schafers, M., 1998. Painful mononeuropathy in C57BL/Wld mice with delayed wallerian degeneration: differential effects of cytokine production and nerve regeneration on thermal and mechanical hypersensitivity. Brain Res. 784, 154–162.
Stankiewicz, A.M., Goscik, J., Swiergiel, A.H., Majewska, A., Wieczorek, M., Juszczak, G. R., Lisowski, P., 2014. Social stress increases expression of hemoglobin genes in mouse prefrontal cortex. BMC Neurosci. 15, 130.
Stankiewicz, A.M., Goscik, J., Majewska, A., Swiergiel, A.H., Juszczak, G.R., 2015. The effect of acute and chronic social stress on the hippocampal transcriptome in mice. PLoS One 10, e0142195.
Starobova, H., Vetter, I., 2017. Pathophysiology of chemotherapy-induced peripheral neuropathy. Front. Mol. Neurosci. 10, 174.
Stephens, K.E., Zhou, W., Ji, Z., Chen, Z., He, S., Ji, H., Guan, Y., Taverna, S.D., 2019. Sex differences in gene regulation in the dorsal root ganglion after nerve injury. BMC Genomics 20, 147.
Summers, D.W., DiAntonio, A., Milbrandt, J., 2014. Mitochondrial dysfunction induces Sarm1-dependent cell death in sensory neurons. J. Neurosci. 34, 9338–9350.
Szretter, K.J., Samuel, M.A., Gilfillan, S., Fuchs, A., Colonna, M., Diamond, M.S., 2009. The immune adaptor molecule SARM modulates tumor necrosis factor alpha production and microglia activation in the brainstem and restricts West Nile virus pathogenesis. J. Virol. 83, 9329–9338.
Turkiew, E., Falconer, D., Reed, N., Hoke, A., 2017. Deletion of Sarm1 gene is neuroprotective in two models of peripheral neuropathy. J. Peripher. Nerv. Syst. 22, 162–171.
Uccellini, M.B., Bardina, S.V., Sanchez-Aparicio, M.T., White, K.M., Hou, Y.J., Lim, J.K., Garcia-Sastre, A., 2020. Passenger mutations confound phenotypes of SARM1-deficient mice. Cell Rep. 31, 107498.
Usoskin, D., Furlan, A., Islam, S., Abdo, H., Lönnerberg, P., Lou, D., Hjerling-Leffler, J., Haeggström, J., Kharchenko, O., Kharchenko, P.V., 2015. Unbiased classification of sensory neuron types by large-scale single-cell RNA sequencing. Nat. Neurosci. 18, 145–153.
Vanni, S., Zattoni, M., Moda, F., Giaccone, G., Tagliavini, F., Haik, S., Deslys, J.P., Zanusso, G., Ironside, J.W., Carmona, M., Ferrer, I., Kovacs, G.G., Legname, G., 2018. Hemoglobin mRNA changes in the frontal cortex of patients with neurodegenerative diseases. Front. Neurosci. 12, 8.
Waller, A.V., 1850. XX. Experiments on the section of the glossopharyngeal and hypoglossal nerves of the frog, and observations of the alterations produced thereby in the structure of their primitive fibres. Philos. Trans. R. Soc. Lond. 423–429.
Walser, M., Schioler, L., Oscarsson, J., Aberg, M.A., Wickelgren, R., Svensson, J., Isgaard, J., Aberg, N.D., 2017. Mode of GH administration and gene expression in the female rat brain. J. Endocrinol. 233, 187–196.
Wang, M., Wu, Y., Culver, D.G., Glass, J.D., 2001. The gene for slow Wallerian degeneration (Wld(s)) is also protective against vincristine neuropathy. Neurobiol. Dis. 8, 155–161.
Wang, M.S., Davis, A.A., Culver, D.G., Glass, J.D., 2002. WldS mice are resistant to paclitaxel (taxol) neuropathy. Ann. Neurol. 52, 442–447.
Wang, Q., Zhang, S., Liu, T., Wang, H., Liu, K., Wang, Q., Zeng, W., 2018. Sarm1/Myd88-5 regulates neuronal intrinsic immune response to traumatic axonal injuries. Cell Rep. 23, 716–724.
Yamamoto, Y., Ueyama, T., Ito, T., Tsuruo, Y., 2015. Downregulation of growth hormone 1 gene in the cerebellum and prefrontal cortex of rats with depressive-like behavior. Physiol. Genomics 47, 170–176.
Young, G.T., Emery, E.C., Mooney, E.R., Tsantoulas, C., McNaughton, P.A., 2014. Inflammatory and neuropathic pain are rapidly suppressed by peripheral block of hyperpolarisation-activated cyclic nucleotide-gated ion channels. Pain 155, 1708–1719.
Yu, P., Liu, Z., Yu, X., Ye, P., Liu, H., Xue, X., Yang, L., Li, Z., Wu, Y., Fang, C., Zhao, Y.J., Yang, F., Luo, J.H., Jiang, L.H., Zhang, L., Zhang, L., Yang, W., 2019. Direct gating of the TRPM2 channel by cADPR via specific interactions with the ADPR binding pocket. Cell Rep. 27 (3684–3695), e3684.